CORRECTION OF THE EFFECT OF RELATIVE WIND DIRECTION ON WIND SPEED DERIVED BY ADVANCED MICROWAVE SCANNING RADIOMETER

Masanori Konda

Department of Geophysics, Kyoto University, Japan, konda@kugi.kyoto-u.ac.jp

Akira Shibata

JAXA/EORC, Japan, shibata.akira@jaxa.jp

ABSTRACT: The sea surface wind speed (SSWS) derived by microwave radiometer can be contaminated by change of microwave brightness temperature owing to the angle between the sensor azimuth and the wind direction (Relative Wind Direction). We attempt to correct the contamination to the SSWS derived by Advanced Microwave Scanning Radiometer (AMSR) on Advanced Earth Observing Satellite II (ADEOS-II), by applying the method proposed by Konda and Shibata (2004). The improvement of accuracy of the SSWS estimation amounts to roughly 60% of the error caused by the RWD effect.

KEY WORDS: AMSR, Relative wind direction, ocean wind, SeaWinds

1. INTRODUCTION

Microwave radiometers contribute to monitoring the sea surface wind speed (SSWS) and its variability. However, there are still some problems in algorithms for the estimation of the SSWS as well as the other geophysical parameters. Several studies (Wentz, 1992; Yueh et al., 1999; Meissner and Wentz, 2002) have pointed out that the brightness temperature (BT) can change according to the angle between the sensor azimuth and the wind direction (relative wind direction, hereafter RWD). The change of the BT due to the RWD allows some errors to creep into the SSWS retrieval. The error approximately amounts to 2-3 ms^{-1} (Wentz, 1997; Konda and Shibata, 2004 , hereafter KS04).

Wentz (1997) firstly took into account this effect (RWD effect) in the operational SSM/I wind retrieval algorithm, where an error curve derived from a harmonic analysis was assumed. However, the error of his analysis is not evaluated well, possibly because of the difficulty in obtaining the footprint of the SSM/I collocated with the ocean vector winds (OVW) under various climatic conditions.

Recently, Konda and Shibata (2004) attempted to evaluate the change of the BT due to the RWD effect, by using SSM/I-derived SSWS collocated with wind vector cells derived by a microwave radar scatterometer, SeaWinds on QuikSCAT. Their analysis is based on the expectation of the high accuracy of the OVW derived by SeaWinds (Ebuchi et al. 2002, Freilich and Vanhoff 2003). They proposed an experimental approach to correct the RWD effect without knowing the information on the wind direction. The approach, using an experimental look-up table, generally succeeded in reducing the error caused by the RWD effect. However, the data used in their study were obtained under limited environmental conditions, because of the orbital difference between SSM/I and QuikSCAT.

Since Advanced Earth Observing Satellite II (ADEOS-II) carried SeaWinds scatterometer as well as Advanced Microwave Scanning Radiometer (AMSR), many collocations for various climatic zones were derived. It enables us to extract the RWD effect experimentally. The simultaneous observations of AMSR and SeaWinds are helpful for preparing a match-up data set, covering various kinds of climatic zones and geographical locations, in order to make up a look-up table.

This paper aims to apply the method proposed by KS04 to the correction of the RWD effect on the AMSR wind and evaluate the improvement by using the simultaneous observation of SeaWinds OVW.

2. DATA AND METHOD

We retrieved the SSWS from the measured BTs provided by Japan Aerospace Exploration Agency (JAXA) in a form of the AMSR level 1B data set. Owing to the limited lifetime of ADEOS-II, we used the observations from April to September 2003, when both AMSR and SeaWinds data were available. Level 1B data consists of the calibrated AMSR BTs, whose footprints are on the swath along the orbit. The wind speed is retrieved basically according to the AMSR standard algorithm, which is the modified algorithm of Shibata (1994) (Shibata 2002). Wind direction is obtained by the level 2B of the OVW data derived by SeaWinds on ADEOS-II.

First, we retrieve the raw AMSR SSWS without the RWD correction (hereafter RAWS) by removing the

module for the correction of the RWD effect from the AMSR standard algorithm. Next, we apply the method of KS04 and evaluate how much the correction is done. The method to correct the RWD effect on the BTs is described in detail in KS04.

In this study, according to KS04, we extract the relationship between the BTs with the vertical ($BT36_V$) and the horizontal polarization ($BT36_H$) at 36.5 GHz. We define the index representing the partial shift of the $BT36_H$ caused by the SSWS (PS36), as the deviation from a linear relationship between the $BT36_V$ and $BT36_H$ under the windless condition (SSWS=0)x ($BBT36|_{SSWS=0}$) (see Figure 2 of KS04).

$$PS36 = \left\langle BT36_H - BBT36|_{SSWS=0} \right\rangle \quad (1)$$

In preparation for the correction procedure, we experimentally established a look-up table correlating PS36 with SST, integrated water vapor (IWV), cloud liquid water (CLW), SSWS, and RWD.

$$PS36_T = PS36(SST, IWV, CLW, SSWS, RWD) , \quad (2)$$

where $PS36_T$ indicates the value in the look-up table.

We use the AMSR level 2B geophysical parameter standard products for SST, IWV, and CLW. The index for the SWSS in the look-up table should be independent of the SeaWinds wind speed, considering the application to the AMSR-E-derived SSWS. We define another index (U6) for the SSWS for the look-up table by applying an algorithm – the same one as that used to derive RAWS - to the BTs at the lowest frequency (6 GHz). It is expected that the BTs are less sensitive to the RWD in the lower frequencies near the incident angle of 55° (Fung and Eom, 1984). U6 is well correlated with the wind speed but has a small bias and a relatively large standard deviation of as much as ±2 ms^{-1}.

The RWD is computed, using the ADEOS-II level 2B swath data for SeaWinds OVW. A spatial difference of up to 12.5 km is allowed as the collocation of the observation cells.

The look-up table obtained by the near-simultaneous observation of AMSR and SeaWinds is used to correct the $BT36_H$. The change of the PS36 in the ranges of geophysical parameters of SST, IWV, CLW and U6 should express the RWD effect appeared in the $BT36_H$.

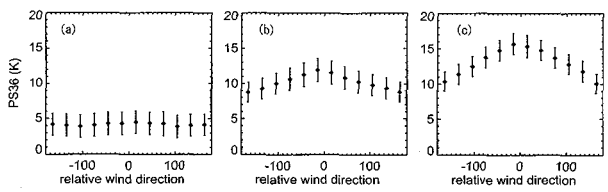

Figure 1: Values of the PS36 at some typical ranges of tropical climate. The ranges of the environmental parameters (SST, IWV, CLW) is (25-27 °C, 40-41 mm, 0-0.02 Kgm^{-2}). The index of the SSWS (U6) increases from (a) 2-3 ms^{-1}, (b) 6-7 ms^{-1}, to (c) 9-10 ms^{-1}. The values are plotted against the RWD. The vertical line in the figure indicates the standard deviation of each value of the PS36.

$$PS36_{TR} = PS36_T(RWD)|_{SST,IWV,CLW,U6} \quad (3)$$

Figure 1 shows examples of the look-up table in a range of the geophysical parameters, which are typical of the tropical climatic zone. By comparing the $PS36_{TR}$ obtained from the look-up table with the PS36 directly obtained by eq.(1), the most appropriate value of $PS36_{TR}$ in the table is determined. The difference between the selected $PS36_{TR}$ and that for the crosswind measurement is considered as the RWD effect on the $BT36_H$. We reduce the value from the raw $BT36_H$ and compute the wind speed again, by using the corrected $BT36_H$.

3. CORRECTION OF THE RWD EFFECT

As indicated in Fig.1, the value of the PS36 depends on the RWD. The dependence is stronger under the high wind speeds than under low winds. Under the high wind speeds, the difference of $PS36_{TR}$ between the upwind and the downwind condition becomes up to 4K as shown in the panel c in Fig.1. This is caused by the inhomogeneous distribution of the slope of ocean facets (Cox and Munk, 1954a; 1954b; Ebuchi and Kizu, 2002).

Now that we have obtained the look-up table, we can correct the AMSR-derived SSWS. Note that we do not use any information on the wind direction for the correction. We apply the RWD correction scheme to the AMSR BTs. Figure 4 shows the difference between the AMSR-derived SSWS with the RWD correction and the SeaWinds-derived SSWS under the cloud-free condition in the tropical climatic zone. Mean differences in the respective ranges of the wind speed are plotted against the RWD. Mean wind speed derived by SeaWinds in each range is shown in individual panels. The result is evaluated by the simultaneously collocated SeaWinds observations. The error of the RAWS is superimposed by the broken line. The contrast of these values seen in Fig.2 clearly indicates the significant reduction of the systematic error caused by the RWD effect.

Figure 2 shows that the RWD effect is strong and the correction works significantly in the high wind condition (panels (b) and (c)). In contrast, the correction hardly

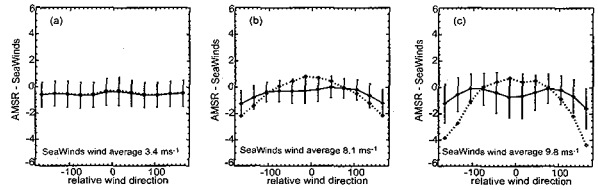

Figure 2: The difference between the AMSR-derived SSWS and the collocated SeaWinds SSWS at the tropical condition. The thick line and diamonds indicate the SSWS, which undergoes the correction of the RWD effect. The broken line indicates the RAWS without the correction. The ranges of the physical parameters are the same as those in Fig. 1. The U6 increases from the left panel to the right, i.e. (a) 2-3 ms^{-1}, (b) 6-7 ms^{-1}, and (c) 9-10 ms^{-1}. The mean SeaWinds SSWS in the individual range is also shown in each panel. The vertical line indicates the standard deviation.

works in the low wind condition, as the RWD effect itself is not significant, compared with the standard deviation (panel (a)). These features are common both in the other climatic conditions. In contrast, the RWD effect becomes the most strong in the cold condition (not shown).

The RWD effect on the wind speed is evaluated by the difference between the maximum and the minimum error. Table 1 shows the result of application of the method according to KS04 together with RAWS in the range of U6 from 9 to 10 ms-1. The strong RWD dependence of the RAWS, which is more than 4.0 ms-1, shows that the RWD effect on the estimation is serious. The improvement indicated in Table 1 shows that as much as 60% of the RWD effect is reduced by the correction used in this study. The climatic condition does not seem to affect the result, although the error reduction is slightly larger in the tropical condition. Table 1 also shows an example of the improvement in the cloudy condition; the error is reduced although the ratio of improvement is smaller than in the cloud-free condition.

4. DISCUSSION AND CONCLUSIONS

We attempted to apply the method proposed by KS04 for the correction of the RWD effect on the SSWS retrieved by AMSR. The RWD was computed by the angle between the sensor azimuth angle of AMSR and the collocated OVW observed by SeaWinds on ADEOS-II. We prepare the PS36T table in terms of SST, IWV,CLW, U6 and RWD in advance of the correction of the RAWS.

In the correction process, we can determine the PS36 from the $BT36_H$ and the $BT36_V$. Then, a $PS36_{TR}$, which is obtained from the look-up table at individual footprints (eq. (3)), nearest to the PS36 obtained from the BTs is chosen as the most appropriate value, according to KS04. The difference between the $PS36_{TR}$ in the cross-wind condition and the selected $PS36_{TR}$ is reduced from the raw $BT36_H$ to obtain the corrected $BT36_H$. Finally, the corrected SWSS is obtained by re-computing with use of the corrected $BT36_H$.

By using the much-up data set with the SeaWinds OVW, as much as 60% of the inaccuracy caused by the RWD effect is reduced in the RAWS derived by AMSR, as shown in Table 1. Results in the different climatic regimes do not change so much. As was pointed out by KS04, the RWD effect is strong in the high wind regime. The correction is successful under the cloudy conditions as well as the cloud-free condition.

The uncertainty of the SSWS estimation should have a serious impact on the computation of the latent heat flux, because the role of the SSWS for the latent heat flux shows a marked increase with the increasing SSWS (Fairall et al. 2003). Therefore, the instantaneous latent heat flux derived by the microwave radiometer suffers from the RWD effect especially at its large value. The correction of the RWD effect on the SSWS should contribute to improvements in monitoring the global distribution and change of the air-sea thermal exchange.

We show the impact of the correction of the RWD effect on the instantaneous estimation of the latent heat flux by contrasting the latent heat fluxes using the SSWS with and without the correction of the RWD effect. As AMSR observes the SST, IWV, and SSWS without a time lag, we obtain the latent heat flux at the footprints of AMSR is possible by using the TOGA-COARE version 2.5B bulk formula for the latent heat (Fairall et al., 1996).

The surface level specific humidity is related to the mixing ratio, which is estimated from the IWV by an experimental equation proposed by Liu and Niiler (1984). is computed with some assumptions about the typical oceanic atmosphere.

Figure 3 shows an example of the density distribution of the relationship between the latent heat flux with and without the correction of the RWD effect during August 2003. Results using data from the other months are almost the same. The difference is evidently enlarged more in the large latent heat flux condition. The impact of the RWD effect grows in proportion to the value of the latent heat flux. The root mean square of the impact of the correction for the latent heat flux is 28.0 Wm^{-2}.

The results of this study indicate that the method proposed by KS04 can be successfully applied to the correction of the systematic error imbedded in the SSWS derived by AMSR. However, there remains some room for improvement. The RWD dependence of PS36 is at most 4-5 K (Fig.1), as that of the BT is as small as 3-4 K at horizontal polarization. Calibration errors of the BT and their temporal drift can influence on the accuracy of the look-up table. Another major possibility is further improvement of the standard products other than the wind speed, as they are needed for the method in this study for establishing and consulting the look-up table. Application

Table 1: The RWD dependence of the estimation error of the SSWS in four typical climate conditions. The results tabulated here are those where the wind speed index U6 is from 9.0 to 10.0 ms-1. The dependence is evaluated by the difference between the maximum and the minimum value of the estimation errors in a range, where the parameters (SST, CLW, IWV, U6) other than the RWD are fixed. The results with and without the correction of the RWD effect are indicated. The SeaWinds wind speed is referred to as the truth data.

	Cold condition[a]	Mid-latitude condition[b]	Tropical condition[c]	Cold-Cloud condition[d]
(maximum - minimum)/standard deviation			9.0< U6 < 10.0	
AMSR				
Raw wind	4.9 / 1.7	4.9 / 1.8	4.6 / 1.7	3.6 / 1.3
With correction	2.2 / 0.7	2.0 / 0.6	1.5 / 0.5	2.0 / 0.7

(a) : SST: 5- 7 C, IWV: 4- 5 mm, CLW : 0-0.02Kgm-1
(b) : SST: 17-19 C, IWV: 14-15 mm, CLW : 0-0.02Kgm-1
(c) : SST: 25-27 C, IWV: 40-41 mm, CLW : 0-0.02Kgm-1
(d) : SST: 3- 5 C, IWV: 13-14 mm, CLW : 0.1-0.12Kgm-1

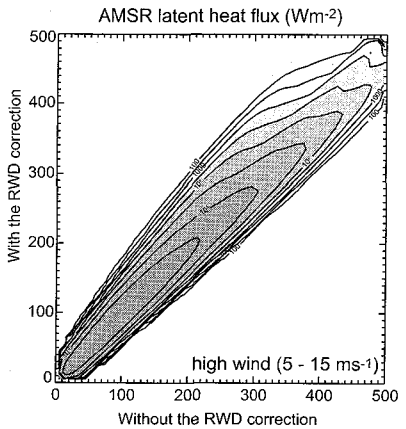

Figure 3: A density distribution of the relationship between the instantaneous latent heat fluxes derived by using the AMSR-derived SSWS with and without the RWD correction during August 2003. The data, whose SSWS with the correction is 5-15 ms^{-1}, are indicated.

of this method to AMSR-E is discussed in Konda et al. (2006).

REFERENCES

Cox, C. and W. Munk, 1954a. Statistics of the sea surface derived from sun glitter. *J. Mar. Res.*, 13, 198-227.

Cox, C. and W. Munk, 1954b. Measurements of the roughness of the sea surface from photographs of the sun's glitter. *J. Opt. Soc. Am.*, 44, 838-850.

Ebuchi, N. and S. Kizu, 2002. Probability distribution of surface wave slope derived using sun glitter images from Geostationary Meteorological Satellite and surface vector winds from scatterometers. *J. Oceanogr.*, 58, 477-486.

Ebuchi, N., H. C. Graber and M. J. Caruso, 2002. Evaluation of wind vectors observed by QuikSCAT/SeaWinds using ocean buoy data, *J. Atmos. Oceanic Technol.*, 19, 2049 – 2062.

Fairall, C. W., E. F. Bradley, D. P. Rogers, J. B. Edson and G. S. Young, 1996. Bulk parameterizations of air-sea fluxes in TOGA COARE. *J. Geophys. Res.*, 101, 3747–3767.

Fairall, C. W., E. F. Bradley, J. E. Hare, A. A. Grachev and J. B. Dobson, 2003. Bulk parameterization of air-sea fluxes: Updates and verification for the COARE algorithm. *J. Climate*, 16, 571-591.

Freilich, M.H. and B.A. Vanhoff, 2003. The relationship between winds, surface roughness, and radar backscatter at low incidence angles from TRMM Precipitation Radar measurements. *J. Atmos. Ocean. Tech.*, 20, 549-562.

Fung, A. K. and H. J. Eom, 1984. A reevaluation of Stogryn's apparent temperature theory over the sea surface. *IEEE Trans. Antennas Propagat.*, 32, 641-643.

Konda, M. and A. Shibata, 2004. An experimental approach to correct the microwave radiometer wind speed affected by the change of the brightness temperature due to the relative wind direction. *Geophys. Res. Lett.*, 31, L09302, doi:10.1029/2004GL019487

Konda, M, A. Shibata, N. Ebuchi and K. Arai, 2006. Correction of relative wind direction on wind speed derived by Advanced Microwave Scanning Radiometer. *J. Oceanogr.*, 62, 395-404

Liu, W.T. and P.P. Niiler, 1984. Determination of monthly mean humidity in the atmospheric surface layer over oceans from satellite data. *J. Phys. Oceanogr.*, 14, 1451-1457

Meissner, T. and F. Wentz, 2002. An updated analysis of the ocean surface wind direction signal in passive microwave brightness temperatures. *IEEE Trans. Geosci. Remote Sens.*, 40, 1230– 1240.

Shibata, A., 1994. Determination of water vapor and liquid water content by an iterative method. *Meteorol. Atmos. Phy.*, 54, 173-181.

Shibata, A., 2002. AMSR/AMSR-E sea surface wind speed algorithm. EORC Bulletin/Technical Report, vol. 9, -Special Issue on AMSR Retrieval Algorithms-, 45 – 46.

Wentz, F. J., 1992. Measurement of Oceanic Wind Vector Using Satellite Microwave Radiometers. *IEEE Trans. Geo. Remote Sens.*, 30, 960 – 972.

Wentz F. J., 1997. A well-calibrated ocean algorithm for SSM/I. *J. Geophys. Res.*, 102,. 8703-8718.

Yueh, S. H., W. J. Wilson, S. J. Dinardo, and F. F. Li, 1999. Polarimetric microwave brightness signatures of ocean wind directions. *IEEE Trans. Geosci. Remote Sens.*, 37, 949– 959.

ACKNOWLEDGMENTS

Level 1B brightness temperature and Level 2 geophysical parameters of AMSR were compiled and provided by Earth Observation Research and application Center, JAXA. SeaWinds on QuikSCAT Level 2B ocean wind vectors in 25 km swath grid of SeaWinds on ADEOS-II (JPL SeaWinds Project) were supplied by the NASA Jet Propulsion Laboratory, PO.DAAC. This study is supported by the Joint Research Program with JAXA "Study of the improvement of the ocean surface wind retrieval algorithm by using the comparison of the collocated brightness temperature and sigma-0" and "Study of the relationship between the relative wind direction and brightness temperatures derived by AMSR and AMSR-E".